



# Enantiomeric resolution, thermodynamic parameters, and modeling of clausenamidone and neoclausenamidone on polysaccharide-based chiral stationary phases

Xuna Luo | Chengqiao Fang | Junru Mi | Jingzi Xu | Hansen Lin

College of Pharmacy, Guangdong Pharmaceutical University, Guangzhou City, Guangdong Province, People's Republic of China

## Correspondence

Hansen Lin, College of Pharmacy, Guangdong Pharmaceutical University, No. 280, East Waihuan Street, Higher Education Mega Center, Panyu District, Guangzhou City, Guangdong Province, People's Republic of China.  
Email: linhansenyd@163.com

## Funding information

Department of Science and Technology of Guangdong Province, Grant/Award Numbers: 2015A020211031 and 2016A020217022; Natural Science Foundation of Jiangsu Province, Grant/Award Number: BK20160032

## Abstract

The aim of the paper is to describe a new synthesis route to obtain synthetic optically active clausenamidone and neoclausenamidone and then use high-performance liquid chromatography (HPLC) to determine the optical purities of these isomers. In the process, we investigated the different chromatographic conditions so as to provide the best separation method. At the same time, a thermodynamic study and molecular simulations were also carried out to validate the experimental results; a brief probe into the separation mechanism was also performed. Two chiral stationary phases (CSPs) were compared with separate the enantiomers. Elution was conducted in the organic mode with n-hexane and iso-propanol (IPA) (80/20 v/v) as the mobile phases; the enantiomeric excess (ee) values of the synthetic *R*-clausenamidone and *S*-clausenamidone and *R*-neoclausenamidone and *S*-neoclausenamidone were higher than 99.9%, and the enantiomeric ratio (er) values of these isomers were 100:0. Enantioselectivity and resolution ( $\alpha$  and  $R_s$ , respectively) levels with values ranging from 1.03 to 1.99 and from 1.54 to 17.51, respectively, were achieved. The limits of detection and quantitation were 3.6 to 12.0 and 12.0 to 40.0  $\mu\text{g/mL}$ , respectively. In addition, the thermodynamics study showed that the result of the mechanism of chiral separation was enthalpically controlled at a temperature ranging from 288.15 to 308.15 K. Furthermore, docking modeling showed that the hydrogen bonds and  $\pi$ - $\pi$  interactions were the major forces for chiral separation. The present chiral HPLC method will be used for the enantiomeric resolution of the clausenamidone derivatives.

## KEYWORDS

chiral chromatographic column, chiral recognition, docking, enantiomeric resolution, HPLC

## 1 | INTRODUCTION

Clausenamide, a kind of pyrrolidone compound, is isolated from an aqueous extract of the leaves of *Clausena lansium*. Based on a pharmacological study, *S*-clausenamide can be used as a liver protectant or nootropic, which is

characterized by improved learning and memory capabilities in normal and memory-impaired rodents,<sup>1,2</sup> and increased the  $[\text{Ca}^{2+}]_i$  concentration to a moderate level.<sup>3</sup> Additionally, clausenamide can stimulate the central cholinergic neurons,<sup>4,5</sup> decrease apoptosis with high phosphorylation of the tau protein, and inhibit long-term

potentiation (LTP) of the synaptic transmission effect,<sup>6</sup> while other enantiomers have resulted in the opposite effect without biological activity. To improve the pharmacokinetic properties and the dissolubility levels of clausenamidone and based on the principle of optimization of the lead compound and the existing research, a series of clausenamidone (CM) derivatives has been designed for synthesis. To provide a preliminary resolution basis for the quality control of CM and neoclausenamidone (NM) derivatives, the determination of the optical purity values of CM and NM was necessary. Optically pure CM and NM have been synthesized before,<sup>7</sup> but in our study, we have explored a simpler and faster method of separation to obtain these compounds. However, how are the optical purity values of these isomers to be determined? According to a previous report,<sup>8</sup> both notations of the enantiomeric excess (ee)<sup>9</sup> and enantiomeric ratio (er)<sup>10</sup> can be found when the enantiomers are quantified by chromatography. On the basis of the IUPAC gold book, for a mixture of (+) and (-)-enantiomers, with the compositions given as the mole or weight fractions of F(+) and F(-) (where F(+) + F(-) = 1), ee is defined as

$F(+)-F(-)$  and ee% as  $100/F(+)-F(-)$ ; the er is defined as the ratio of the percentage of one enantiomer in a mixture to that of the other, eg, 70 (+):30 (-).<sup>11</sup> In this regard, the er is the normalized ratio (proportion) as it is directly measured by the chromatographic peak area.

Moreover, the separation process of the chiral stationary phases (CSPs) under different chromatographic conditions was also investigated, and the results of separation were validated by modeling and thermodynamics research.

## 2 | MATERIALS AND METHODS

### 2.1 | Chemicals and reagents

Racemic CM and NM were first synthesized according to Rao EC,<sup>12</sup> and then (-)-menthyloxyacetic acid was used as the chiral resolving agent to obtain CM and NM in their enantiomerically pure forms (Figure 1).

Compared with an earlier report, although (-)-menthyloxyacetic acid was also used as the resolving

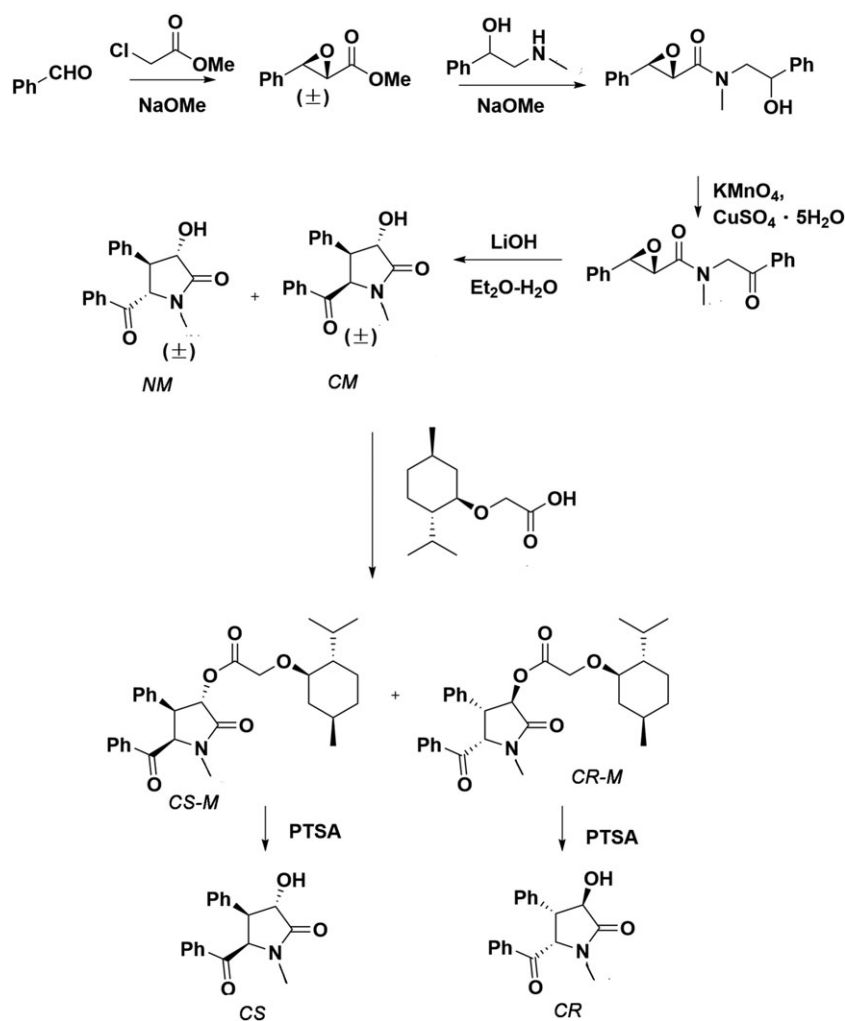


**FIGURE 1** The synthesis of *R*-clausenamidone and *S*-clausenamidone and *R*-neoclausenamidone and *S*-neoclausenamidone

agent, the process used a highly toxic agent such as pyridine, and the reaction lasted longer than 10 hours. We used the classic esterification method with *N,N'*-dicyclohexylcarbodiimide (DCC) and 4-dimethylaminopyridine (DMAP) directly, and the process could be completed in 1 hour. The chiral separation process was as follows (CM is taken as example): To a solution of racemic CM in dichloromethane, DCC, DMAP, and (–)-menthylxyacetic acid were added. After stirring at room temperature for 1 hour, the reaction mixture was filtered off from the insoluble substances. Then, the solvent was removed, and the solid residue left behind was separated by column chromatography and purified by recrystallization with methanol. Two diastereomers as white crystals were obtained, and hydrolysis of the two diastereomers provided *S*-clausenamidone (CS) and *R*-clausenamidone (CR) (Figure 2). The chiral separation of NM was the same process as of that of CM to provide *S*-neoclausenamidone (NS), and *R*-neoclausenamidone (NR).

## 2.2 | Characterization data

CM: white crystal, melting point (m.p.) 208.1 to 209.7°C, <sup>1</sup>H NMR (500 MHz, chloroform-*d*) δ 7.56 to 7.50 (m, 2H), 7.41 (ddt, *J* = 8.7, 7.3, 1.3 Hz, 1H), 7.30 to 7.20 (m, 2H), 7.14 to 7.09 (m, 2H), 7.09 to 7.02 (m, 2H), 7.04 to 6.97 (m, 1H), 5.40 (d, *J* = 8.9 Hz, 1H), 4.95 to 4.89 (m, 1H), 3.87 (t, *J* = 9.4 Hz, 1H), 3.55 (d, *J* = 2.7 Hz, 1H), 2.89 (d, *J* = 0.6 Hz, 3H); HRMS (ESI): *m/z* [M + H]<sup>+</sup>, calculated: 296.1281, found: 296.1283.

CS: white crystal, m.p. 196.6 to 198.4°C, [α]<sub>20</sub> D – 340.2 (*c* = 0.5 g/cm<sup>3</sup> in CH<sub>3</sub>OH), <sup>1</sup>H NMR (500 MHz, chloroform-*d*) δ 7.56 to 7.50 (m, 2H), 7.41 (ddt, *J* = 8.7, 7.3, 1.3 Hz, 1H), 7.30 to 7.20 (m, 2H), 7.14 to 7.09 (m, 2H), 7.09 to 7.02 (m, 2H), 7.04 to 6.97 (m, 1H), 5.40 (d, *J* = 8.9 Hz, 1H), 4.95 to 4.89 (m, 1H), 3.87 (t, *J* = 9.4 Hz, 1H), 3.55 (d, *J* = 2.7 Hz, 1H), 2.89 (s, 3H); HRMS (ESI): *m/z* [M + H]<sup>+</sup>, calculated: 296.1281, found: 296.1283.

CR: white crystal, m.p. 198.9 to 200.5°C, [α]<sub>20</sub> D + 312.5 (*c* = 0.5 g/cm<sup>3</sup> in CH<sub>3</sub>OH), <sup>1</sup>H NMR (500 MHz, chloroform-*d*) δ 7.56 to 7.50 (m, 2H), 7.44 to 7.37 (m, 1H), 7.27 to 7.20 (m, H), 7.15 to 7.09 (m, 2H), 7.09 to 7.03 (m, 2H), 7.03 to 6.97 (m, 1H), 5.40 (d,

*J* = 8.9 Hz, 1H), 4.92 (dd, *J* = 9.8, 2.9 Hz, 1H), 3.87 (t, *J* = 9.4 Hz, 1H), 3.55 (d, *J* = 2.9 Hz, 1H), 2.89 (s, 3H); HRMS (ESI): *m/z* [M + H]<sup>+</sup>, calculated: 296.1281, found: 296.1284.

NM: white crystal, m.p. 192.1 to 194.7°C, <sup>1</sup>H NMR (300 MHz, chloroform-*d*) δ 7.71 to 7.62 (m, 2H), 7.62 to 7.48 (m, 1H), 7.32 (td, *J* = 9.5, 8.5, 3.6 Hz, 5H), 7.28 to 7.15 (m, 2H), 5.10 (d, *J* = 6.6 Hz, 1H), 4.55 (d, *J* = 6.6 Hz, 1H), 4.37 (s, 1H), 3.31 (t, *J* = 6.6 Hz, 1H), 2.94 (s, 3H); HRMS (ESI): *m/z* [M + H]<sup>+</sup>, calculated: 296.1281, found: 296.1279.

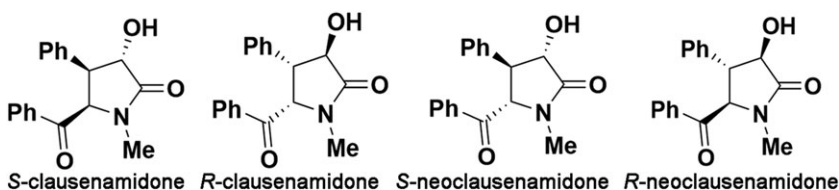
NS: white crystal, m.p. 182.8 to 185.7°C, [α]<sub>20</sub> D – 14.0 (*c* = 1 g/cm<sup>3</sup> in CH<sub>3</sub>OH); <sup>1</sup>H NMR (300 MHz, chloroform-*d*) δ 7.72 to 7.15 (m, 10H), 5.10 (d, *J* = 6.5 Hz, 1H), 4.51 (d, *J* = 6.6 Hz, 1H), 3.30 (t, *J* = 6.6 Hz, 1H), 4.14(d, *J* = 6.6 Hz, 1H)2.95 (s, 3H); HRMS (ESI): *m/z* [M + H]<sup>+</sup>, calculated: 296.1281, found: 296.1283.

NR: white crystal, m.p. 182.1 to 184.7°C, [α]<sub>20</sub> D + 14.5 (*c* = 1 g/cm<sup>3</sup> in CH<sub>3</sub>OH); <sup>1</sup>H NMR (300 MHz, chloroform-*d*) δ 7.73 to 7.63 (m, 2H), 7.61 to 7.49 (m, 1H), 7.40 to 7.17 (m, 7H), 5.10 (d, *J* = 6.6 Hz, 1H), 4.52 (d, *J* = 6.6 Hz, 1H), 4.14(q, *J* = 6.6 Hz, 1H), 3.32 (t, *J* = 6.6 Hz, 1H), 2.96 (s, 3H); HRMS (ESI): *m/z* [M + H]<sup>+</sup>, calculated: 296.1281, found: 296.1276.

## 2.3 | Chromatographic conditions

The enantiomeric separations were conducted on a high-performance liquid chromatography (HPLC) system (model 1200 series, Agilent Technology) equipped with a quaternary pump, online degasser, autosampler, column oven, and diode array detector (DAD). Two CSPs, CHIRALPAK AD-H based on amylose derivatized with tris-(3,5-dimethylphenyl carbamate) (25 cm × 4.6 mm I. D., 5 μm) and CHIRALCEL OJ-H based on cellulose derivatized with tris-(4-methylbenzoate) (25 cm × 4.6 mm I.D., 5 μm), were evaluated in this study. These chiral columns were purchased from Daicel Chiral Technologies (China) Co. Ltd. The mobile phase was a mixture of *n*-hexane and iso-propanol (IPA). By using 1.0 mL/min as the flow rate, the injection volume was 20 μL, and the detection wavelength was 254 nm. Chromatography variables such as the retention (*k*), separation (*α*), and resolution (*R<sub>s</sub>*) factors were determined. 1,3,5-Tri-*tert*-butylbenzene was used to calculate the dead time. The

**FIGURE 2** The structures of *R*-clausenamidone and *S*-clausenamidone and *R*-neoclausenamidone and *S*-neoclausenamidone



determinations of the optical purities of CS, CR, NS, and NR were conducted using the best separation method which was based on the investigation of the different chromatographic conditions to provide the ee% and er values, where the computational methods were as follows: for example, CR (ee%) =  $100/F(+)-F(-)$ , where F(+) represents the peak area % of CR and F(-) represents the peak area % of CS. The CM er value represents the ratio of the peak area % of CR and the peak area % of CS, that is F(+):F(-).

## 2.4 | Method validation

According to a previous report, the validation of the proposed method was characterized by the following parameters: specificity, accuracy, precision, limit of detection (LOD) and limit of quantification (LOQ), and linearity.<sup>13</sup>

## 2.5 | Simulation studies

With the ever-growing power of computers, software, and computer graphics (to display structures along with their physicochemical properties), molecular modeling has become a practical tool for evaluating more complex interactions such as those of the associations between chiral selectors and selectants.<sup>14</sup> Computer modeling was conducted with Autodock4.2. The ligands used were CM and NM, while the receptors were the amylose and cellulose stationary phases with 12 units<sup>15</sup> (Figure 3). ChemDraw was applied to sketch the structures of CM

and NM; then, these two structures were converted with Chem3D to obtain the minimal energy structures. After that, Autodock4.2 (ADT) was used to process the structures of the receptors and ligands, which were then saved in PDBQT files. A lattice box size of  $60 \text{ \AA} \times 60 \text{ \AA} \times 60 \text{ \AA}$  with a spacing of  $0.371 \text{ \AA}$  was used. After docking, the output files were opened in Discovery Studio 4.5 to obtain the image of molecular docking interaction.

## 3 | RESULTS AND DISCUSSION

### 3.1 | Chromatographic data

The HPLC measurements of the retention (k), separation ( $\alpha$ ), and resolution (Rs) were ascertained for the enantiomers of CM and NM on amylose derivatized with tris-(3,5-dimethylphenyl carbamate) and cellulose derivatized with tris-(4-methylbenzoate) CSPs. The magnitudes of the racemic CM and NM contents are given in the Table 1, which indicated that the retention (k) and resolution (Rs) would decrease with increasing fraction of IPA. It could be concluded that interaction between the sample and stationary phase weakened as the IPA content was increased. The order of separated peaks of HPLC is shown in Figure 4 with the 80/20 (v/v) n-hexane/IPA mobile phase at a temperature of 298.15 K.

### 3.2 | Investigation of the thermodynamic parameters

Thermodynamic experiments were carried out in the range of 288.15 to 308.15 K, and the results are given in Table 2 and Figure 5. In the chromatographic separation of the enantiomers, the Gibbs free energy change  $\Delta G^\ominus$  was measured, which represents the binding energy between the CSPs and the samples.  $\Delta G^\ominus$  can be calculated at a constant temperature according to the Gibbs-Helmholtz equation 1. In addition, the relation between the chromatographic retention and temperature can be described by the Van't Hoff equations 2 and 3, where  $\Delta H^\ominus$  and  $\Delta S^\ominus$  represent the change in the standard molar enthalpy and standard molar entropy, respectively,  $\Delta\Delta H^\ominus$  and  $\Delta\Delta S^\ominus$  represent the difference in the standard molar enthalpy change and in the standard molar entropy change between the stationary phase and mobile phase, respectively, R is the universal gas constant ( $8.3144 \text{ J}/[\text{mol}\cdot\text{K}]$ ), and T is the absolute temperature (K). The enantiomeric bonding is greatly driven by intermolecular interactions as measured by the enthalpy change  $\Delta H^\ominus$ . The process of complexation is usually reflected by the entropic cost  $\Delta S^\ominus$ .<sup>16</sup> The thermodynamic values were calculated using Origin2018.

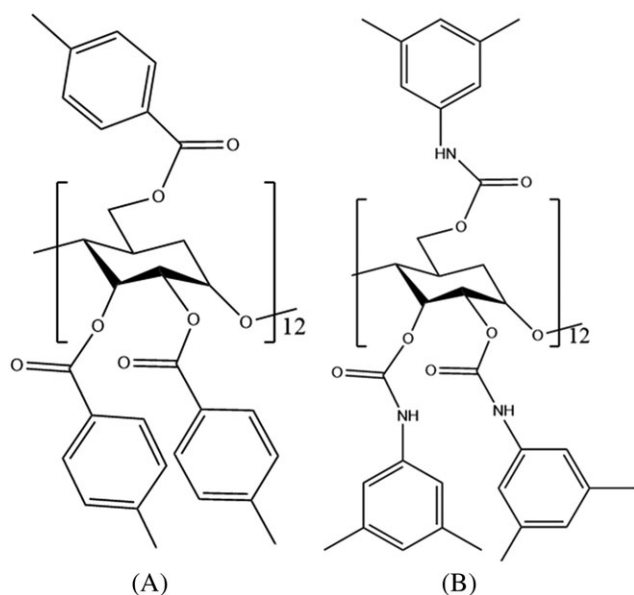


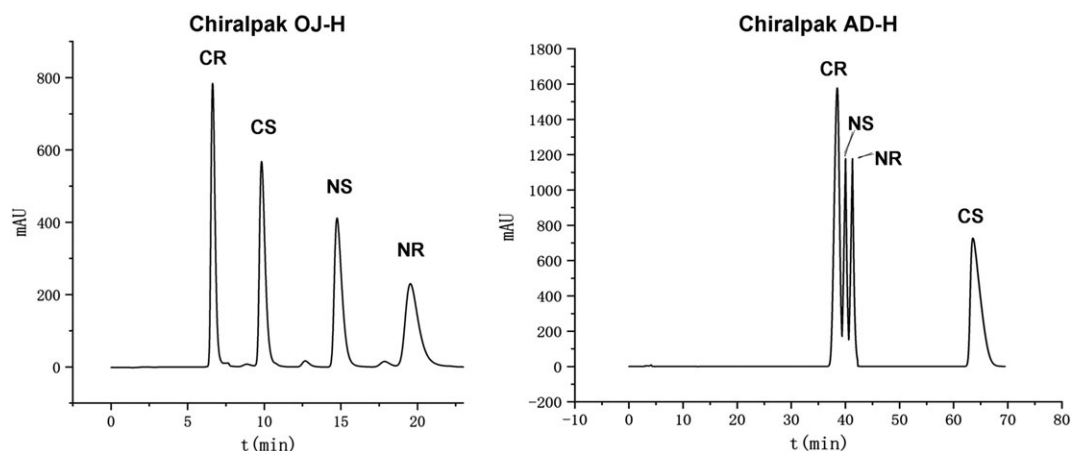
**FIGURE 3** A, 2D structure of the tris-(4-methylbenzoate) cellulose chiral selector. B, 2D structure of the tris-(3,5-dimethylphenyl carbamate) amylose chiral selector

**TABLE 1** Results of separation of racemic clausenamidone and neoclausenamidone on the Chiralcel OJ-H and Chiralpak AD-H columns

Compound	Column (CSP)	Mobile Phase (v/v)	$\kappa_1$	$\kappa_2$	$\alpha$	Rs
Clausenamidone	Chiralcel OJ-H	n-hexane/IPA 90/10	2.86	5.70	1.99	13.58
		n-hexane/IPA 85/15	1.63	3.15	1.93	11.53
		n-hexane/IPA 80/20	1.03	1.97	1.91	9.01
	Chiralpak AD-H	n-hexane/IPA 90/10	11.99	18.66	1.56	16.76
		n-hexane/IPA 85/15	6.20	10.00	1.61	16.26
		n-hexane/IPA 80/20	4.10	6.80	1.66	16.06
Neoclausenamidone	Chiralcel OJ-H	n-hexane/IPA 90/10	7.77	13.04	1.68	14.57
		n-hexane/IPA 85/15	4.30	6.83	1.59	11.56
		n-hexane/IPA 80/20	2.93	4.04	1.38	7.08
	Chiralpak AD-H	n-hexane/IPA 90/10	11.74	12.27	1.05	1.54
		n-hexane/IPA 85/15	6.44	6.63	1.03	0.95

Abbreviation: IPA, iso-propanol.

The temperature of the column was at 298.15 K.

**FIGURE 4** Chiral resolutions of clausenamidone and neoclausenamidone on the Chiralcel OJ-H and Chiralpak AD-H columns using n-hexane/IPA (80/20 v/v) as the mobile phase at 298.15 K on Chiralcel OJ-H and n-hexane/IPA (90:10 v/v) as the mobile phase at 298.15 K on Chiralpak AD-H**TABLE 2** Effect of the column temperatures of Chiralcel OJ-H and Chiralpak AD-H on clausenamidone

Column (CSP)	Temperature, K	Clausenamidone			Neoclausenamidone		
		$\kappa_1$	$\kappa_2$	$\alpha$	$\kappa_1$	$\kappa_2$	$\alpha$
Chiralcel OJ-H	288.15	1.27	2.50	1.96	4.76	7.57	1.59
	293.15	1.18	2.29	1.94	4.04	6.21	1.53
	298.15	1.07	2.06	1.92	3.69	5.40	1.46
	300.15	1.09	2.08	1.91	3.49	5.13	1.47
	303.15	1.04	1.97	1.90	3.12	4.43	1.42
	308.15	0.97	1.82	1.88	2.93	4.04	1.38
Chiralpak AD-H	288.15	4.93	10.14	2.06	15.37	16.23	1.06
	293.15	4.79	9.30	1.94	14.07	14.83	1.05
	298.15	4.42	8.19	1.85	12.77	13.41	1.05
	301.15	4.17	7.48	1.80	11.99	12.52	1.04
	303.15	4.17	7.33	1.76	11.74	12.27	1.05
	308.15	4.10	6.80	1.66	10.75	11.16	1.04

<sup>a</sup>The mobile phase was 80/20 (v/v) n-hexane/IPA.

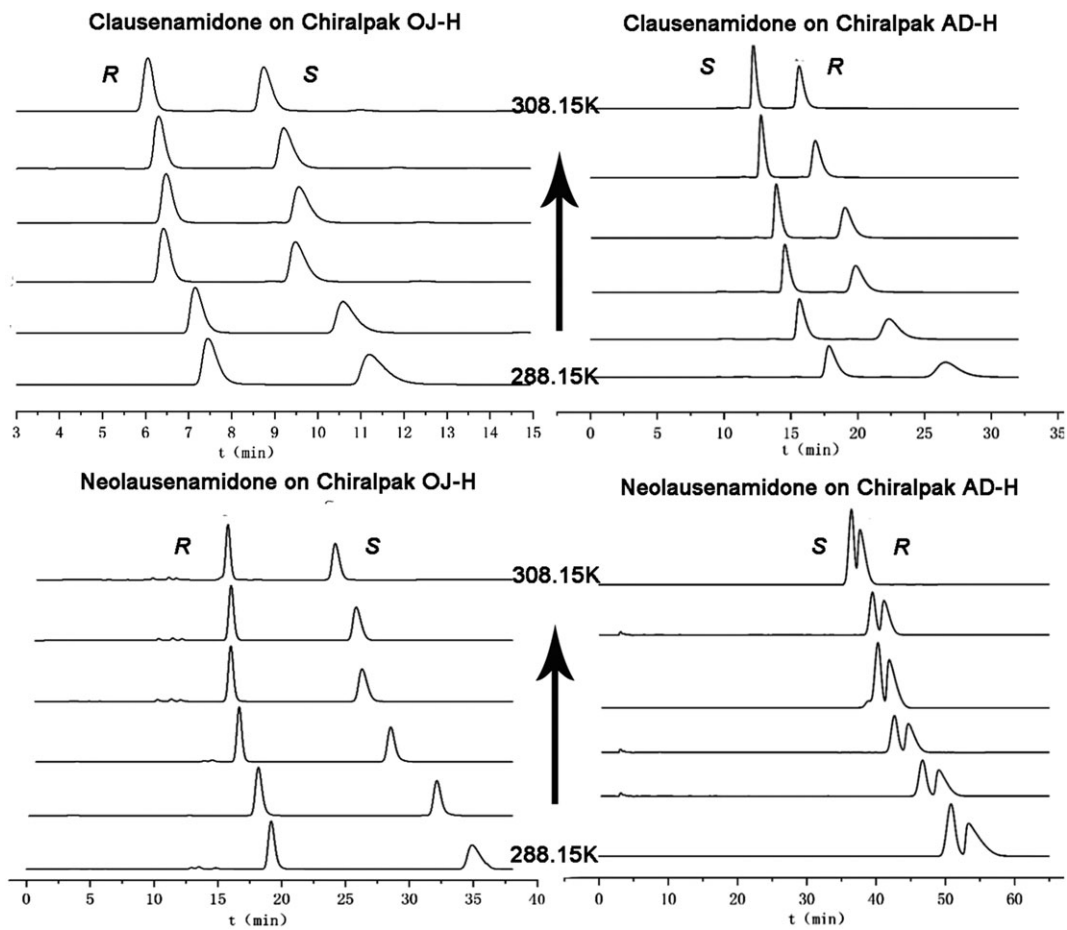


**FIGURE 5** Effect of the column temperature on clausenamidone and neoclausenamidone

$$\Delta G^\ominus = \Delta H^\ominus - T\Delta S^\ominus \quad (1)$$

$$\ln K = -\frac{\Delta H^\ominus}{RT} + \Delta S^\ominus/R \quad (2)$$

$$\ln \alpha = -\Delta \Delta G^\ominus/RT = \frac{\Delta \Delta H^\ominus}{RT} + \Delta \Delta S^\ominus/R \quad (3)$$

As shown in the Table 2, the retention times and retention ( $k$ ) and separation ( $\alpha$ ) factors of the two enantiomers of these two compounds exhibited downward trends from 288.15 to 308.15 K, indicating that the interaction between the sample and stationary phase weakened as the temperature was increased, which was related to the Van't Hoff equation 2. The temperature was raised to facilitate the processes of adsorption and desorption between the solute and the stationary phase. The separation of the chromatogram parameters was a reflection of the reduction in the capacity factor  $k$  and the separation factor  $\alpha$ . Thus, the relation between the chromatographic retention and column temperature could be described by Van't Hoff plots to obtain the linear plots of  $\ln k$  versus  $1/T$  and  $\ln \alpha$  versus  $1/T$ ; the date of the latter linear plots is given in Tables 3 and 4. It was

**TABLE 3** Thermodynamic parameters of clausenamidone (at 298.15 K)

Parameter	R	S	R	S
Column (CSP)	Chiralcel OJ-H		Chiralpak AD-H	
Slope	1299.3	1496.5	937.1	1868.8
Intercept	-4.26	-4.27	-1.66	-4.17
$R^2$	0.96	0.97	0.94	0.99
$\Delta H^\ominus$	-10.80	-12.44	-7.79	-15.54
$\Delta S^\ominus$	-0.04	-0.04	-0.01	-0.03
$\Delta G^\ominus$	-0.25	-1.87	-3.69	-6.60
$\Delta \Delta H^\ominus$ (kJ/mol)	-1.64		-7.75	
$\Delta \Delta S^\ominus$	-0.0001		-0.0209	
$\Delta \Delta G^\ominus$ (kJ/mol)	-1.62		-1.52	
Tiso (K)	22930.23		370.66	

observed that the linear plots of  $\ln k$  versus  $1/T$  and  $\ln \alpha$  versus  $1/T$  had regression coefficients  $R^2 \geq 0.90$  for both compounds. From the Van't Hoff plots, the values of  $\Delta H^\ominus$ ,  $\Delta S^\ominus$ ,  $\Delta \Delta H^\ominus$ ,  $\Delta \Delta S^\ominus$ , and  $\Delta \Delta G^\ominus$  were thus calculated, and the thermodynamic parameters for the chiral separations are provided in Tables 3 and 4.

**TABLE 4** Thermodynamic parameters of neoclausenamidone (at 298.15 K)

Parameter	R	S	R	S
Column (CSP)	Chiralcel OJ-H		Chiralpak AD-H	
Slope	2821.1	2179.4	1675.2	1599.6
Intercept	-7.79	-6.02	-3.03	-2.82
R <sup>2</sup>	0.99	0.98	0.99	0.99
$\Delta H^\ominus$	-23.46	-18.12	-13.93	-13.30
$\Delta S^\ominus$	-0.07	-0.05	-0.03	-0.02
$\Delta G^\ominus$	-4.16	-3.19	-6.42	-6.31
$\Delta\Delta H^\ominus$ (kJ/mol)	-5.34		-0.63	
$\Delta\Delta S^\ominus$	-0.015		-0.002	
$\Delta\Delta G^\ominus$ (kJ/mol)	-0.96		-0.12	
Tiso (K)	363.94		365.75	

using n-hexane/IPA (80/20 v/v) as the optimum mobile-phase composition

The  $\Delta\Delta H^\ominus$  and  $\Delta\Delta S^\ominus$  data in Tables 3 and 4 both exhibited negative values, which indicated that the chiral separation of CM and NM was somewhat enthalpically controlled under the chromatographic conditions. When  $\Delta\Delta H^\ominus$  and  $\Delta\Delta S^\ominus$  were both negative, the second-eluted enantiomer fit much better in the cavity of the selector, thereby forming a more stable complex than in the case of the first-eluted enantiomer; the negative entropy was less favorable for enantioseparation. The enantioseparation was enthalpically driven, as was common, and the selectivity decreased with increasing temperature.<sup>17</sup>

Moreover, according to Equation 2, when the value of separation ( $\alpha$ ) was 1, the corresponding temperature Tiso was obtained, which meant that  $Tiso = \Delta\Delta H^\ominus / \Delta\Delta S^\ominus$ ; the contributions of the enthalpy and entropy in the chiral separation process were offset. When the column temperature was below Tiso, the separation would decrease as the temperature was increased. When the column temperature was Tiso, the isomers would be eluted simultaneously. However, if the column temperature was higher than Tiso, the elution order of the enantiomers would be reversed, and the mechanism of chiral separation would be entropically controlled.<sup>18</sup>

For CM, the values of  $Tiso = \Delta\Delta H^\ominus / \Delta\Delta S^\ominus = 22\,930$  K on Chiralcel OJ-H and  $Tiso = \Delta\Delta H^\ominus / \Delta\Delta S^\ominus = 371$  K on Chiralpak AD-H showed that if the temperatures were below 22 930 K on Chiralcel OJ-H or below 371 K on Chiralpak AD-H, the value of separation ( $\alpha$ ) would decrease as the temperature increased. For NM, the values of  $Tiso = \Delta\Delta H^\ominus / \Delta\Delta S^\ominus = 363$  K on Chiralcel OJ-H and  $Tiso = \Delta\Delta H^\ominus / \Delta\Delta S^\ominus = 365$  K on Chiralpak AD-H showed that if the temperatures were below 363 K on

Chiralcel OJ-H or below 365 K on Chiralpak AD-H, the value of separation ( $\alpha$ ) would decrease as the temperature was increased. Given that a high temperature would damage the column, the verification experiments were not carried out.

In addition, as reported<sup>19</sup> before, when the absolute value of  $\Delta\Delta H^\ominus$  was lower than 0.1 KJ/mol, the chiral recognition was only attributed to the steric hindrance and did not include other types of forces. In the range of 0.5 to 1.0 kJ/mol, the contribution of the steric hindrance was amplified by weak interactions such as the weak  $\pi$ - $\pi$  action, weak hydrogen bonding action, and the like. When the absolute value of  $\Delta\Delta H^\ominus$  was higher than 1.0 kJ/mol, it was considered that the postpeak isomer was subjected to an additional strong  $\pi$ - $\pi$  action or strong hydrogen bonding, which showed somewhat strong chiral recognition levels. For CM, the value obtained by Chiralcel OJ-H was  $\Delta\Delta H^\ominus = -1.64$  kJ/mol and that by Chiralpak AD-H was  $\Delta\Delta H^\ominus = -7.75$  kJ/mol, which reflected strong  $\pi$ - $\pi$  interactions or hydrogen bonding with the CSPs resulting in chiral separation. For NM, the value obtained by Chiralcel OJ-H was  $\Delta\Delta H^\ominus = -5.34$  kJ/mol, which indicated strong  $\pi$ - $\pi$  interactions or hydrogen bonding with the CSPs resulting in chiral separation. However, on Chiralpak AD-H, the value was  $\Delta\Delta H^\ominus = -0.63$  kJ/mol, which was in the range of 0.5 to 1.0 kJ/mol, thereby indicating that the contribution of steric hindrance was amplified by weak interactions such as the weak  $\pi$ - $\pi$  action, weak hydrogen bonding action, and the like.

Thus, it was concluded that when the temperature was below 363 K, the enantioseparation of these samples was enthalpically driven, and according to the thermodynamic parameters, the  $\pi$ - $\pi$  and hydrogen bonding actions were the major interactions between the samples and the CSPs.

### 3.3 | Method validation

#### 3.3.1 | System suitability

HPLC suitability testing was performed using six replicate injections ( $n = 6$ ) of the standard solution (1000  $\mu\text{g/mL}$ ) and the tailing factor, % relative standard deviation (RSD) of the peak area, and % RSD of the retention time were deemed suitable as shown in Table 5.

#### 3.3.2 | Specificity

Specificity of the method was evaluated for any interference by other peaks along with the main peaks. The eluent was loaded onto the machine as a blank. No peak was

**TABLE 5** The results of the method validation

Method Validation			CR	CS	NS	NR
System suitability	Tailing factor		0.59	0.55	0.55	0.59
	Resolution		-	5.01	5.64	3.79
	% RSD peak area		0.90	0.07	0.05	0.14
	% RSD retention time		0.15	0.27	0.33	0.53
Linearity	Slope		40402	38502	33167	31621
	Y-intercept		698.13	465.05	394.97	326.26
	Regression coeff. ( $R^2$ )		0.9996	0.9992	0.9992	0.9993
LOD and LOQ	LOD ( $\mu\text{g/mL}$ )		3.6	4.8	6.0	12.0
	LOQ ( $\mu\text{g/mL}$ )		12.0	16.0	20.0	40.0
Accuracy (percentage recovery data)	CR (300 $\mu\text{g/mL}$ ) CS, NS, NR (350 $\mu\text{g/mL}$ )		1.04	1.03	1.02	1.04
			1.01	1.00	0.98	1.03
			1.02	1.00	0.98	1.03
	CR (330 $\mu\text{g/mL}$ ) CS, NS, NR (440 $\mu\text{g/mL}$ )		0.99	0.99	1.00	1.00
			0.99	0.99	1.00	0.99
			0.99	0.99	1.00	1.00
	CR (450 $\mu\text{g/mL}$ ) CS, NS, NR (570 $\mu\text{g/mL}$ )		0.99	1.00	1.01	1.01
			0.99	1.00	1.01	1.01
		1.00	0.99	0.99	1.01	
Precision (% RSD)	120 $\mu\text{g/mL}$	A <sup>a</sup>	0.07	0.37	0.62	0.38
		T <sup>a</sup>	0.06	0.54	0.10	0.71
	240 $\mu\text{g/mL}$	A	0.93	0.60	0.19	0.40
		T	0.10	0.07	0.11	0.10
	400 $\mu\text{g/mL}$	A	0.62	0.31	0.99	0.25
		T	0.07	0.08	0.06	0.16

<sup>a</sup>A represents the peak area; T represents the retention time.

observed from the blank solution. The latter indicated the specificity of the system.

### 3.3.3 | Linearity

Linearity was evaluated by regression analysis of the curve. The linearity values of the standardized peak areas vs concentrations for all four enantiomers were tested in the 80 to 400  $\mu\text{g/mL}$  concentration range. The slopes, y-intercepts, and regression coefficients ( $R^2$ ) were calculated. These values are given in Table 5. The regression coefficients of the establishment were 0.9992 to 0.9996 for the four enantiomers ( $n = 6$ ).

### 3.3.4 | LOD and LOQ

The LOD and LOQ values were calculated as signal-to-noise ratios of 3 and 10, respectively. The LODs of CR, CS, NS, and NR were 3.6, 4.8, 6.0, and 12  $\mu\text{g/mL}$ , respectively. The LOQs of CR, CS, NS, and NR were 12, 16, 20, and 40  $\mu\text{g/mL}$ , respectively. The % RSD values of the peak areas for the LOD were 0.66 to 0.99. Similarly, the % RSD of the peak areas for the LOQ were 0.62 to 0.84.

### 3.3.5 | Accuracy

The accuracy was determined by calculating the recovery from the spike amounts, and the percent recoveries were found to be in the range of 97.88% to 103.94% for all four enantiomers at three different spiked concentrations (300–570  $\mu\text{g/mL}$ ) as shown in Table 5. This array indicated a high accuracy of the method.

### 3.3.6 | Precision

The precision was determined by three concentrations of all of the enantiomers (120, 240, and 400  $\mu\text{g/mL}$ ) ( $n = 3$ ). The % RSDs of the retention times and peak area were 0.06 to 0.71 and 0.07 to 0.62, respectively, which indicated a suitably precise HPLC method.

## 3.4 | Determination of the optical purity

It could be concluded that the best separation condition of racemic CM and NM was n-hexane/IPA (80/20 v/v) at 298.15 K using Chiralcel OJ-H according to Sections 3.1 and 3.2. Based on this condition, racemic CM and NM were used as the reference objects to determine the

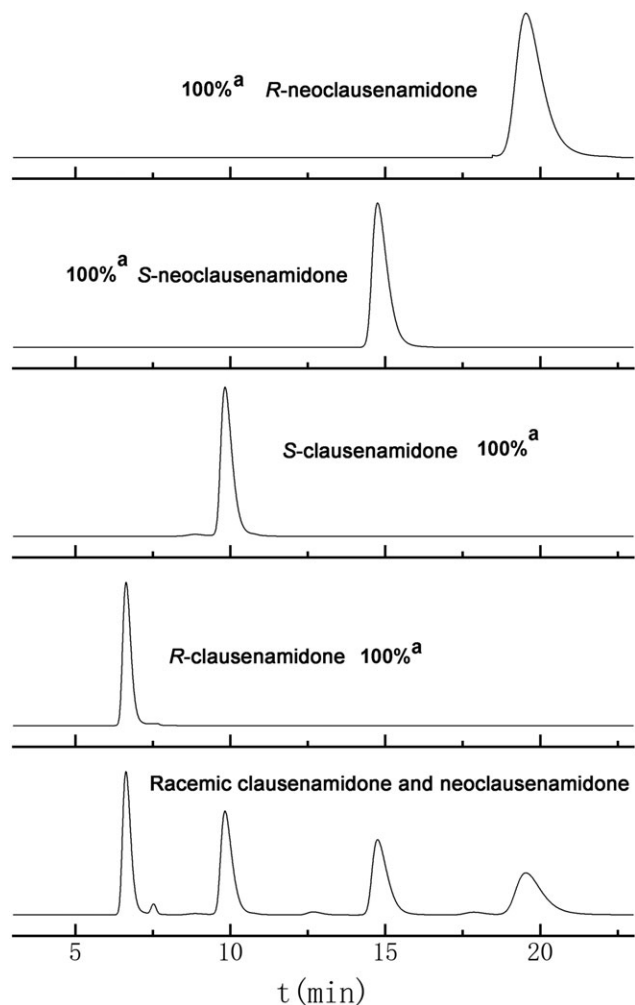


**FIGURE 6** Chiral resolutions of racemic clausenamidone and neoclausenamidone and enantiomers on Chiralcel OJ-H using n-hexane/IPA (80/20 v/v) as the mobile-phase composition at 298.15 K. a. % peak area

optical purities of CS, CR, NS, and NR. The results are shown in Figure 6, which indicated that the ee and the er values for the synthetic CM and NM were higher than 99.9% and 100:0, respectively.

### 3.5 | Simulation studies

The earlier reports<sup>20-26</sup> clearly were in support of chiral recognition being controlled by hydrogen bonding, and hydrophobic,  $\pi$ - $\pi$ , steric interactions, etc. For example, the interactions between the  $\pi$ - $\pi$  stacked and hydrogen bonds are clearly shown between *S*-clausenamidone and CSP with tris-(4-methylbenzoate) cellulose in Figure 7.

In Section 3.1 it was concluded that the interaction between the sample and stationary phase was strengthened as the ratio of IPA decreased, which corresponded to the docking result that the separation was controlled by the hydrogen bonds. Iso-propanol functioned as the proton donor providing hydrogen atoms to form hydrogen bonds with the hydrogen atom of sample. If the IPA in the mobile phase was reduced, the hydrogen bond interaction between IPA and enantiomer would be relatively weakened, and the hydrogen bond force between the CSP and the enantiomer would be strengthened given the long retention time.

From the comparison between the different columns, CM and NM had longer retention times in Chiralpak AD-H with tris-(3,5-dimethylphenyl carbamate) amylose than those in Chiralcel OJ-H with tris-(4-methylbenzoate) cellulose. These results corresponded to the report<sup>27</sup> in which the phenylcarbamate moiety attached to the amylose backbone exhibited a rather high enantiomer resolving ability. It could be explained by the structure of Chiralpak

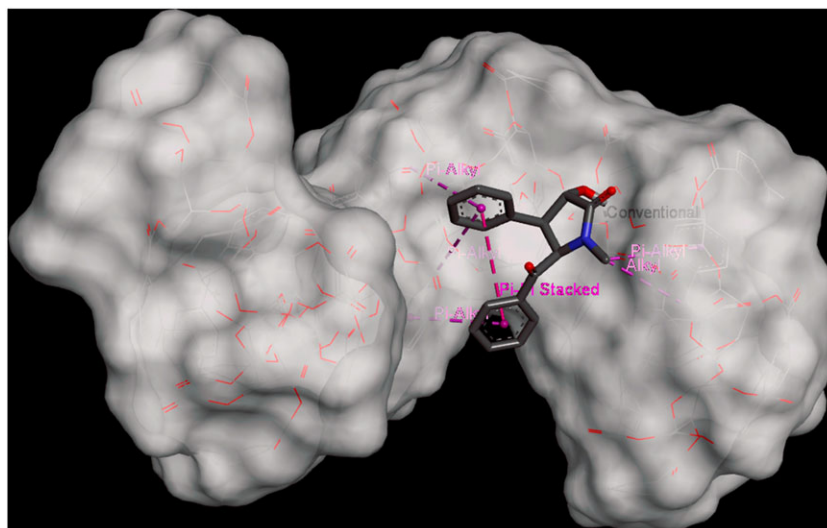


**FIGURE 7** Docking model of *S*-clausenamidone with the tris-(4-methylbenzoate) cellulose chiral selector

AD-H, which has been reported to be a left-handed four-fold (4/1) helix on the basis of X-ray analysis.<sup>28</sup> The carbamate residue formed a large number of grooves around the main chain, and the interaction between the sample and the stationary phase included ammonia hydrogen bond interactions (or dipole-dipole interactions), clathrations, and  $\pi$ - $\pi$  interactions. The strongest chiral adsorption positions of Chiralcel OJ-H were only the carbonyl group, which had formed hydrogen bond interactions, and the phenyl group through  $\pi$ - $\pi$  interactions with aromatic compounds to complete the chiral recognition. Hence, the interaction between the compound and Chiralpak AD-H was stronger than that between the compound and Chiralcel OJ-H. Moreover, the elution time in Chiralpak AD-H was longer than that in Chiralcel OJ-H.

## 4 | CONCLUSION

This study describes the synthesis of optically active CM and NM and discusses their enantioseparations using two different polysaccharide-based CSPs, namely, Chiralcel OJ-H and Chiralpak AD-H. The best separation condition was n-hexane/IPA (80/20 v/v) at 298.15 K using Chiralcel OJ-H; the enantioselectivity and resolution ( $\alpha$  and  $R_s$ , respectively) values were 1.90 and 1.38, and 9.06 and 7.08, respectively. Based on this condition, the ee values were higher than 99.9% and the er values were 100:0 for all synthetic optically active CM and NM. Meanwhile, all of the isomers were separated successfully within 25 minutes, and all validation parameters showed acceptable results; hence, the developed method was efficiently used for the quantitative determination of the enantiomeric purities of the optically active CM and NM. In addition, according to the results of the thermodynamic parameters, it could be concluded that the separation of racemic CM and NM was somewhat enthalpically controlled. At the same time, the results showed that the  $\pi$ - $\pi$  interactions and hydrogen bonding with the CSPs resulted in chiral separation, which corresponded to the results of docking modeling. In all, the described method was successful for evaluating the enantiomers of CM and NM and is of great reference significance for future research on CM and NM and their derivatives.

## ACKNOWLEDGMENTS

This study was supported by the Department of Science and Technology of Guangdong Province (2015A020211031 and 2016A020217022) and the Natural Science Foundation of Jiangsu Province (BK20160032).

## ORCID

Xuna Luo  <https://orcid.org/0000-0003-3115-0258>

## REFERENCES AND NOTES

1. Zhang J, Cheng Y, Zhang JT. Protective effect of (-) clausenamide against neurotoxicity induced by okadaic acid and beta-amyloid peptide25–35[J]. *Yao xue xue bao Acta pharmaceut Sinica*. 2007;42(9):935-942.
2. Tang K, Zhang JT. (-) clausenamide improves long-term potentiation impairment and attenuates apoptosis after transient middle cerebral artery occlusion in rats[J]. *Neurol Res*. 2003;25(7):713-717.
3. Duan W, Zhang J. Effects of (-),(+) clausenamide on anisodine-induced acetylcholine decrease and associated memory deficits in the mouse brain[J]. *Yao xue xue bao Acta pharmaceut Sinica*. 1998;33(4):259-263.
4. Bayer AJ, Bullock R, Jones RW, et al. Evaluation of the safety and immunogenicity of synthetic A $\beta$ 42 (AN1792) in patients with AD[J]. *Neurology*. 2005;64(1):94-101.
5. Selkoe DJ. Alzheimer's disease is a synaptic failure[J]. *Science*. 2002;298(5594):789-791.
6. Li XZ, Lai K, Wu KM, Huang DF, Huang L. Studies on the synthesis and biological evaluation of the metabolite of clausenamide CM2 and its stereoisomers[J]. *Eur J Med Chem*. 2014;74:736-741.
7. Hansen L. Resolution of neoclausenamidone[J]. *Acad J Guangdong Coll Pharma*. 1999;2.
8. Tiritan ME, Fernandes C, Maia AS, Pinto M, Cass QB. Enantiomeric ratios: why so many notations?[J]. *J Chromatogr A*. 2018;1569:1-7.
9. Han J, Kitagawa O, Wzorek A, Klika KD, Soloshonok VA. The self-disproportionation of enantiomers (SDE): a menace or an opportunity?[J]. *Chem Sci*. 2018;9(7):1718-1739.
10. Sriyatep T, Tantapakul C, Andersen RJ, et al. Resolution and identification of scalemic caged xanthenes from the leaf extract of *Garcinia propinqua* having potent cytotoxicities against colon cancer cells[J]. *Fitoterapia*. 2018;124:34-41.
11. Book G. Compendium of chemical terminology[J]. *Int Union Pure Appl Chem*. 2014;528.
12. Rao EC, Hong H, Cheng JC, Yang GZ. Total synthesis of clausenamide[J]. *Chin Chem Lett*. 1994;5:267-267.
13. Ali I, Khattab RA, Alothman ZA, Badjah AY, Alwarthan A. Enantiomeric resolution and modeling of DL-alanine-DL-tryptophan dipeptide on amylose stationary phase[J]. *Chirality*. 2018;30(4):491-497.
14. Lämmerhofer M. Chiral recognition by enantioselective liquid chromatography: mechanisms and modern chiral stationary phases[J]. *J Chromatogr A*. 2010;1217(6):814-856.
15. Ye YK, Bai S, Vyas S, Wirth MJ. NMR and computational studies of chiral discrimination by amylose tris (3, 5-dimethylphenylcarbamate)[J]. *J Phys Chem B*. 2007;111(5):1189-1198.
16. Wani DV, Rane VP, Mokale SN. Liquid chromatographic separation and thermodynamic investigation of lorcazerin

- hydrochloride enantiomers on immobilized amylose-based chiral stationary phase[J]. *Chirality*. 2018;30(3):284-292.
17. Lajkó G, Orosz T, Kiss L, et al. High-performance liquid chromatographic enantioseparation of fluorinated cyclic  $\beta$ -amino acid derivatives on polysaccharide-based chiral stationary phases. Comparison with nonfluorinated counterparts[J]. *Biomed Chromatogr*. 2016;30(9):1441-1448.
  18. Stringham RW, Blackwell JA. Factors that control successful entropically driven chiral separations in SFC and HPLC[J]. *Anal Chem*. 1997;69(7):1414-1420.
  19. Küsters E, Spöndlin C. Influence of temperature on the enantioseparation of rolipram and structurally related racemates on Chiracel-OD[J]. *J Chromatogr A*. 1996;737(2):333-337.
  20. Morris GM, Goodsell DS, Halliday RS, et al. Automated docking using a Lamarckian genetic algorithm and an empirical binding free energy function[J]. *J Comput Chem*. 1998;19(14):1639-1662.
  21. Ali I, Alam SD, Al-Othman ZA, Farooqi JA. Recent advances in SPE-chiral-HPLC methods for enantiomeric separation of chiral drugs in biological samples[J]. *J Chromatogr Sci*. 2013;51(7):645-654.
  22. Ali I, Saleem K, Hussain I, Gaitonde VD, Aboul-Enein HY. Polysaccharides chiral stationary phases in liquid chromatography[J]. *Sep Purif Rev*. 2009;38(2):97-147.
  23. Aboul-Enein HY, Ali I. *Applications of Polysaccharide-Based Chiral Stationary Phases for Resolution of Different Compound Classes*[M]//chiral separations. Humana Press; 2004:183-196.
  24. Aboul-Enein HY, Ali I. Optimization strategies for HPLC enantioseparation of racemic drugs using polysaccharides and macrocyclic glycopeptide antibiotic chiral stationary phases[J]. *Il Farmaco*. 2002;57(7):513-529.
  25. Aboul-Enein HY, Ali I. Studies on the effect of alcohols on the chiral discrimination mechanisms of amylose stationary phase on the enantioseparation of neбиволol by HPLC[J]. *J Biochem Biophys Methods*. 2001;48(2):175-188.
  26. Ali I, Sanagi MM, Aboul-Enein HY. Advances in chiral separations by nonaqueous capillary electrophoresis in pharmaceutical and biomedical analysis[J]. *Electrophoresis*. 2014;35(7):926-936.
  27. Chankvetadze B, Kartoziya I, Yamamoto C, Okamoto Y. Comparative enantioseparation of selected chiral drugs on four different polysaccharide-type chiral stationary phases using polar organic mobile phases[J]. *J Pharm Biomed Anal*. 2002;27(3-4):467-478.
  28. Okamoto Y, Kaida Y. Resolution by high-performance liquid chromatography using polysaccharide carbamates and benzoates as chiral stationary phases[J]. *J Chromatogr A*. 1994;666(1-2):403-419.

**How to cite this article:** Luo X, Fang C, Mi J, Xu J, Lin H. Enantiomeric resolution, thermodynamic parameters, and modeling of clausenamidone and neoclausenamidone on polysaccharide-based chiral stationary phases. *Chirality*. 2019;1-11. <https://doi.org/10.1002/chir.23068>